

April 1997

MZ-TH/96-36
hep-th/9612010

Weight Systems from Feynman Diagrams

Dirk Kreimer^{*†}*Dept. of Physics
Mainz University
55099 Mainz
Germany*

Abstract

We find that the overall UV divergences of a renormalizable field theory with trivalent vertices fulfil a four-term relation. They thus come close to establish a weight system. This provides a first explanation of the recent successful association of renormalization theory with knot theory.

1 Introduction

Recently, ideas spread to connect knot theory with renormalization theory [1, 2]. This was guided by the observation that overall counterterms are independent of external parameters like masses and momenta. This well-known fact can be cast in a different form: that the only way to change the value of an overall divergence is to change the topology of the diagram, once the spin and other representations of the involved particles are specified. Hence one should not be too surprised if one finds topological information in the numbers which specify the overall divergences. And indeed, meanwhile evidence in abundance reports on a beautiful and unexpected connection between field theory [3, 4, 5, 6, 7], knot theory [8, 9] and number theory [10, 11, 12, 13].

On the one hand these results successfully explore the proposed connection by empirical calculations, while on the other hand an explanation why it works is missing. The connection between field theory and number theory is given by solid calculus, the connection between field theory and knot theory via momentum routings is fairly intuitive [1], and finally the connection between knot and number theory, which the results in [3, 5, 8, 9, 10] so urgently suggest, is still to be found.

In this paper, we will study four-term relations. Such relations appear in a totally different context, related to knot theory via Vassiliev invariants and their study in terms of chord diagrams [14].

^{*}supported by DFG

[†]email: kreimer@dipmza.physik.uni-mainz.de

Here we want to derive the presence of a four-term relation in divergent contributions extracted from Feynman diagrams. In a companion paper, we will present calculations which provide examples for the ideas proposed here [15].

Such a four-term relation (4TR) is a relation between trivalent graphs. It is thus perfectly well suited to help us with our main problem: how to relate trivalent Feynman graphs to knot diagrams.

The presence of a 4TR provides an algebraic structure which directly relates overall counterterms of Feynman diagrams to knot theory. This, we hope, will provide the first and major step in a formal derivation of the relation between renormalization theory and knot theory. The 4TR relation is intimately connected to chord diagrams. Such chord diagrams were envisaged to play a role for our purposes in [1] and were also investigated in [16]. While we disagree with the prescriptions used in [16], since they quickly lead to violations of established connections between knots and transcendentals from counterterms [1], the intent of that work formed some of the motivation for the present analysis.

The paper is organized as follows. In the next section we will motivate the four-term relation and the role it plays in the study of knot invariants of finite type. Our presentation follows [14] closely. Having convinced ourselves that the presence of a four-term relation is the major ingredient to establish algebraic structures which relate to knot theory, we then derive in the main section the presence of a 4TR in the counterterms of overall divergent diagrams in a renormalizable field theory. In the final section we consider a curious example, extending the consideration to the presence of non-renormalizable couplings. We derive a relation, which we will report to be fulfilled in a different paper [15].¹

In this first approach to the subject, we will restrict ourselves to graphs free of subdivergences. We do expect that the general case will be a modification of the results obtained here, but will reserve a more general study for the future.

2 The four-term relation

Let us first define a chord diagram. Strictly following [14], we define:

Definition 1 *A chord diagram is an oriented circle with finitely many chords on it, regarded up to orientation preserving diffeomorphisms of the circle.*

Here, a chord is a pair of distinct points on the circle, connected by a propagator. In [14], one then continues to consider the class of all chords, filtered in a natural manner by the number of chords (which is one less than the number of loops in the diagram). Adopting the notation of [14], we call the set of all diagrams having m chords $\mathcal{G}_m\mathcal{D}^c$.

One of the fundamental results in [14] is the fact that the vector space of Vassiliev invariants is equivalent to the graded space of all weight systems. A weight system is more or less determined by the existence of a 4TR in chord diagrams:

Definition 2 *A real-valued weight system of degree m is a function $W: \mathcal{G}_m\mathcal{D}^c \rightarrow \mathbf{R}$ such that*

¹Actually, this relation was postdicted after David Broadhurst proved the 4TR to fail in its naive form in graphs with non-renormalizable vertices, and I was forced to explain this failure.

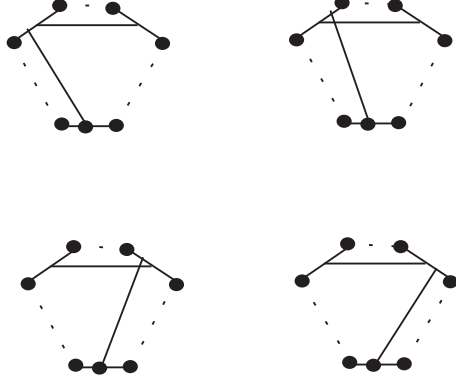


Figure 1: The four-term relation. The alternating sum of the four diagrams $\mathcal{G}_{1,\dots,4}$ vanishes. Note that lines solely specify the topology of the diagram, and not the nature of the particles involved. Dotted lines may be connected in arbitrary ways by further propagators in the same manner for all four diagrams, with the restriction that all four graphs are free of subdivergences.

- i) If $D \in \mathcal{G}_m \mathcal{D}^c$ has an isolated chord, then $W(D) = 0$.
- ii) Whenever four diagrams D_1, \dots, D_4 differ only as shown in Fig.(1), their weights satisfy

$$W(D_1) - W(D_2) + W(D_3) - W(D_4) = 0. \quad (4TR) \quad (1)$$

An isolated chord can be considered as a one-loop subdivergence at the circle.

For our purposes, property *i*) is thus trivially fulfilled.² Property *ii*) is called the four term relation (4TR). Let us denote by \mathcal{W} the space of all weight systems. Then the before-mentioned theorem says that \mathcal{W} is equivalent to the filtered space of Vassiliev invariants over \mathbf{R} . To understand what this means let us consider knots which have m selfintersections, cf. Fig.(2). Let us call the space of all knots with m



Figure 2: This is a knot with two selfintersections. Any knot invariant V can be lifted to a knot invariant on knots with selfintersections.

selfintersections \mathcal{K}_m for the moment.

²This is consistent with the results in [1], which relate iterated one-loop subdivergences to an increasing writhe number, and thus establish a framing dependence. The absence of subdivergences guarantees framing independence, which is the sole purpose of property *i*) in [14].

Assume some knot invariant V is given. We then make it into an invariant of knots with selfintersections by setting

$$V(\times) = V(\times) - V(\times). \quad (2)$$

Resolving all selfintersections with help of this equation iteratively defines the knot invariant on \mathcal{K}_m , $\forall m$. A knot invariant is called an invariant of type m if it vanishes for knots with more than m selfintersections.

$$K \in \mathcal{K}_i, i > m \Rightarrow V(K) = 0. \quad (3)$$

A knot invariant which is of finite type for some $m \in \mathbf{N}$ is called a Vassiliev invariant. The important point about Vassiliev invariants is that all the coefficients of the relevant knot polynomials, like the Conway, Jones, HOMFLY or Kauffman polynomials, are invariants of finite type.

These results show the importance of a 4TR. Once a mapping from trivalent graphs G_i to \mathbf{R} is given which fulfils the 4TR on chord diagrams, we can make it into a weight system by defining a new mapping which vanishes on diagrams with isolated chords, and get from the weight system a Vassiliev knot invariant.

The problem we address in this paper can be stated as follows: counterterms of Feynman diagrams assign to each Feynman graph, considered as a trivalent graph, a (Laurent-) series in a regularization parameter with coefficients in \mathbf{R} .³ For graphs free of subdivergences this is in fact a single number, specifying the overall divergence of the graph. For such graphs condition *i*) in the definition of a weight system is trivially fulfilled. What remains to be checked is the 4TR.

Before we start with our investigation of this problem, we mention some more facts valid for diagrams which fulfil a 4TR. We stress some interesting results from [14] and point out which aspects might be interesting for the calculation of Feynman diagrams. A more detailed discussion will be contained in [17].

- It can be shown that the space of all chord diagrams fulfilling a 4TR is equivalent to the space of all diagrams fulfilling a STU-relation, which is a three-term relation. We shall attempt to investigate the STU relation in the future. If it can be established as well, arbitrary Feynman diagrams can be reduced to Feynman diagrams which can be written as chord diagrams.
- The resulting algebra of diagrams provides a naturally defined product and co-product, which makes it into a commutative and cocommutative Hopf algebra. Such algebraic structures, once identified in overall divergent counterterms, might turn out to be useful in future calculations.
- It is reasonably conjectured that all weight systems come from Lie algebras [14]. If this is true their algebraic relations should be reflected in overall divergent counterterms. If this in turn is wrong, our overall counterterms might provide the first example of a weight system which does not come from Lie algebra.⁴

³We are only interested in the proper divergent part of this series.

⁴At this point, it might be interesting to know how big these spaces of diagrams really are,

3 Overall divergences and 4TR

The idea which we want to pursue combines field theory and topology. On the one hand, we learned that symbolic graphs which are related by a 4TR establish weight systems. On the other hand we know from previous work that the overall counterterms of Feynman diagrams are connected to knot theory. So far, this was obtained as an empirical fact, by establishing a knot-to-number dictionary.

Now, we want to come closer to an explanation of this phenomenon by establishing a 4TR between the overall divergences of Feynman graphs. Our input are Feynman graphs which will be shown to be related by a 4TR. For a start, we exclude cases which contain subdivergences. A short glance at the Dyson-Schwinger equations ensures that this restricts ourselves to vertex corrections. Further, as we work with a renormalizable (but not super-renormalizable) theory, we will conclude that the graphs to be considered have logarithmic degree of divergence.

In such a case, we can calculate the overall divergence by nullifying all external masses and momenta in all propagators. We then assume that we can cut the diagram at appropriate places, and find the overall divergence of a n -loop graph as the finite part of a $(n - 1)$ -loop two-point function.

In so doing, we assume that the cutting is legitimate. This restricts ourselves to places where we can cut without generating IR divergences. As we see below, the derivation of the 4TR determines where we must be able to cut the graphs. This restricts the class of available graphs. In future work we will discuss modifications of the 4TR which can incorporate such cases as well.

Also, in a parallel paper, we will present an explicit 4-loop calculation which establishes the 4TR as proposed here, and demonstrates its failure in cases when our derivation is not applicable [15].

We now want to prove that Feynman diagrams fulfil a four-term relation (4TR).

Theorem 1 (4TR) *Four Feynman graphs \mathcal{G}_i , $i = 1, \dots, 4$, of logarithmic degree of divergence, which fulfil*

- i) that they are free of subdivergences (skeleton diagrams),*
- ii) that they are related as in Fig.(1),*
- iii) that the propagators connecting x_m to x_i with vertices V_i at x_i , $i \in \{l, r\}$, fulfil $\Delta_F(s)V_i = V_i\Delta_F(s)$ for any constant vector s ,⁵*
- iv) that the propagators connecting $x_a - x_l, x_b - x_l, x_c - x_r, x_d - x_r$ have no form-factor of tensor rank two,⁶*

for increasing loop number. Interestingly, row 3, table 6.1 in [14] gives numbers which seem intimately related but not identical to the number of distinct irreducible MZVs [18] found in overall counterterms of graphs with appropriate loop number [9, 17]. To compare entries of table 1 in [9] with [14], add in row M_n the entry for odd n to the (even) entry for $n - 1$, starting from $n = 5$. The first disagreements occur at $n = 15$ and $n = 19$.

⁵A vector boson coupling to a fermion thus would not fulfil this condition, for example: $\not{s}\gamma_\mu - \gamma_\mu\not{s} \neq 0$.

⁶ Thus, scalar particles, fermions and gauge bosons in the Feynman gauge pose no problem. If we have zero momentum couplings at a fermion line we might be in trouble, see below. Constraints *iii)* and *iv)* may be relaxed when one allows for modifications of the 4-term relation.

v) that they provide a correction to a dimensionless coupling constant of a renormalizable theory,⁷

fulfil

$$< \mathcal{G}_1 - \mathcal{G}_2 + \mathcal{G}_3 - \mathcal{G}_4 > = 0. \quad (4)$$

To prove this theorem, we use contour integrals. We start with contour integrals which vanish by the residue theorem. But, as we will argue, they pick up the coefficients of the overall divergence of the four Feynman diagrams above, as their sole divergent contribution.

Our guiding philosophy is the following. Assume that all internal momentum integrations are cut-off by an appropriate λ . Then, all our contour integrals to be defined below exist. We then collect all terms which will diverge for $\lambda \rightarrow \infty$ after addition of all the contours. We will find that the remaining divergent contributions establish the 4TR as envisaged in the theorem.

Hence we will shortly define ten contour integrals I_i , $i = 1, \dots, 10$, with ten contours Γ_i , which fulfil

$$I_i = 0, \quad \forall i \in 1, \dots, 10; \quad (5)$$

because the contours are closed rectangles, and the functions to be integrated are analytic inside these rectangles.

Each contour Γ_i consists of four paths $\gamma_{i,j}$, $j = 1, \dots, 4$. The contributions from these individual paths are denoted by $I_{i,j}$. We then show that

$$0 = < \sum_{i=1}^{10} \sum_{j=1}^4 I_{i,j} > = < I_{1,2} + I_{5,2} + I_{6,2} + I_{10,2} >, \quad (6)$$

where the first equality follows from Eq.(5), while the second equality has to be proved. Finally, we will find that

$$\begin{aligned} < I_{1,2} > &= < \mathcal{G}_1 >, \\ < I_{10,2} > &= - < \mathcal{G}_2 >, \\ < I_{6,2} > &= < \mathcal{G}_3 >, \\ < I_{5,2} > &= - < \mathcal{G}_4 >, \end{aligned} \quad (7)$$

which proves the theorem. Here, $< \dots >$ denotes projection onto the divergent part of the expression in the brackets. This projection can be done in various ways. For our purposes, it is sufficient to cut the last momentum integration. The brackets then project onto the coefficients of the singularity present in the final momentum integration.

To proceed, we have to introduce some more notation. First, note that for space-time points (coordinates) we will use variables from the end of the alphabet: x, y, z , where we might use alpha-numerical subscripts to denote more of them, like in x_0, x_a, \dots, x_m . They are Lorentz vectors in space-time, where we usually omit to give the Lorentz indices, but, if needed, denote them by greek sub(super)scripts. We use a four-dimensional Euclidean metric, supposing that Wick rotation

⁷In a renormalizable theory with only trivalent couplings, provisos *i*) and *v*) are not independent. We include *v*) as we will extend our considerations to more general cases in the course of this paper.

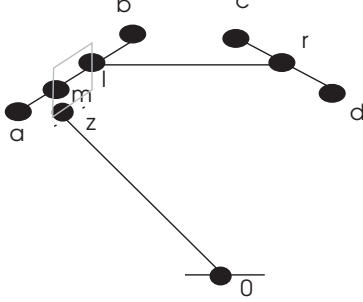


Figure 3: The endpoint z of the propagator $\Delta_F(x_0 - z)$ moves around a contour which lies in the extension of the parallel space $x_m - x_l$ to a complex plane. This figure refers to the case \mathcal{G}_1 , where x_m is located between x_a and x_l . Similar figures hold for the other cases.

is performed *ab initio* in Eqs.(8-11) below. Unit vectors will be denoted by a caret, for example $\hat{y}_\mu := y_\mu / \sqrt{y^2}$, where $y^2 = y_\mu y^\mu$. The modulus of a vector is denoted by $\bar{y} := \sqrt{y^2}$.

For momenta we will use letters from the middle of the alphabet, k, l, m, \dots, r . Occasionally, we will use the notation $k \cdot y = k_\parallel \bar{y}$, where $k_\parallel := k \cdot \hat{y}$. Here, $k \cdot y$ denotes the scalar product $k_\mu y^\mu$.

In Fig.(3) we now define the relevant propagators and vertices. We specify 9 points: $x_a, x_b, x_c, x_d, x_0, x_l, x_r, x_m$ and z , as indicated in the Fig.(3). All differences between the four graphs of Fig.(1) can be specified by the propagators which connect the points $(x_0, x_m, x_a, x_b, x_c, x_d, x_l, x_r)$.

The propagators of Fig.(3) correspond to one part of the analytic expression for the diagrams \mathcal{G}_i . The rest is contained in a function $\mathcal{G}(x_a, x_b, x_c, x_d, x_0)$, which is universal for all four diagrams.

These four diagrams \mathcal{G}_i can now be written as⁸

$$\mathcal{G}_1 := \int dX \mathcal{G}(x_a, x_b, x_c, x_d, x_0) \Delta_F(x_r - x_l) \Delta_F(x_0 - x_m) \Delta_F(x_m - x_a) \Delta_F(x_l - x_m) \Delta_F(x_b - x_l) \Delta_F(x_r - x_c) \Delta_F(x_d - x_r), \quad (8)$$

$$\mathcal{G}_2 := \int dX \mathcal{G}(x_a, x_b, x_c, x_d, x_0) \Delta_F(x_r - x_l) \Delta_F(x_0 - x_m) \Delta_F(x_l - x_a) \Delta_F(x_m - x_l) \Delta_F(x_b - x_m) \Delta_F(x_r - x_c) \Delta_F(x_d - x_r), \quad (9)$$

$$\mathcal{G}_3 := \int dX \mathcal{G}(x_a, x_b, x_c, x_d, x_0) \Delta_F(x_r - x_l) \Delta_F(x_0 - x_m) \Delta_F(x_l - x_a) \Delta_F(x_b - x_l) \Delta_F(x_m - x_c) \Delta_F(x_r - x_m) \Delta_F(x_d - x_r), \quad (10)$$

$$\mathcal{G}_4 := \int dX \mathcal{G}(x_a, x_b, x_c, x_d, x_0) \Delta_F(x_r - x_l) \Delta_F(x_0 - x_m) \Delta_F(x_l - x_a) \Delta_F(x_b - x_l) \Delta_F(x_r - x_c) \Delta_F(x_m - x_r) \Delta_F(x_d - x_m). \quad (11)$$

In all four \mathcal{G} functions the propagator $\Delta_F(x_0 - x_m)$ appears. It will be the endpoint

⁸For simplicity, we drop all factors coming from vertices. We will comment on vertices later.

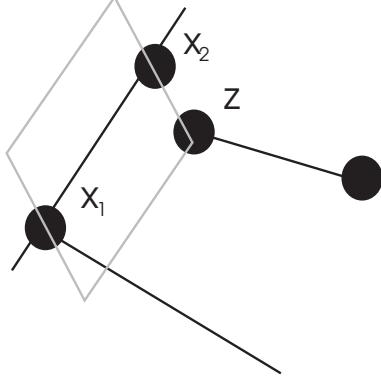


Figure 4: The generic case for all our contour integrals. Here, $y = x_1 - x_2$.

x_m of this propagator which will be the subject of a contour integration.

$\mathcal{G}(x_a, x_b, x_c, x_d, x_0)$ incorporates the five-point function which corresponds to all other not specified propagators and vertices in the Feynman diagrams. It is the same function in all four cases. $\int dX$ summarizes the integration over all internal vertices, $\int d^4x_a \dots \int d^4x_m$. There might be other internal vertices in $\mathcal{G}(x_a, x_b, x_c, x_d, x_0)$, whose integration is always understood. We do not specify where external particles couple, but in principle allow them to couple anywhere. As we are interested only in the overall divergence, we nullify masses and external particles in all propagators. As mentioned before, we assume that this can be done without introducing IR problems.

We also use the Fourier transform $\tilde{\Delta}_F(k)$

$$\Delta_F(y) =: \int d^4k \tilde{\Delta}_F(k) e^{ik \cdot y}. \quad (12)$$

Now we introduce the contour integrations which we have in mind. We use

$$\oint_{\Gamma(y)} dz e^{izk \cdot \hat{y}} = 0, \quad \forall k, y. \quad (13)$$

The contour $\Gamma(y)$ is a contour in a complex plane. The real axis of this complex plane is identified as a multiple of the vector \hat{y}_μ . This unit vector defines a one-dimensional real space, which we extend to a one-dimensional complex space. Further, $\Gamma(y)$ is a rectangle with corners $-i\epsilon, \bar{y} - i\epsilon, \bar{y} + i\epsilon, i\epsilon$, with negative orientation, cf. Fig.(4). ϵ is a fixed strictly positive real parameter, which need not be small. This being said, Eq.(13) is obvious.

Next, we define the parametrization of $\Gamma(y)$ by four functions $f_i(u, k, y; \rho, \epsilon)$

$$\begin{aligned} \oint_{\Gamma(y)} dz e^{izk \cdot \hat{y}} &\equiv \sum_{i=1}^4 \int_{l_i}^{u_i} du f_i(u, k, y; \rho, \epsilon) \\ f_1(u, k, y; \rho, \epsilon) &:= e^{ik \cdot \hat{y}(u - i\epsilon)}, \quad l_1 = \rho \bar{y}, \quad u_1 = \bar{y}, \\ f_2(u, k, y; \rho, \epsilon) &:= e^{ik \cdot \hat{y}(\bar{y} + ui)}, \quad l_2 = -\epsilon, \quad u_2 = \epsilon, \end{aligned}$$

$$\begin{aligned}
f_3(u, k, y; \rho, \epsilon) &:= -e^{ik \cdot \hat{y}(u+i\epsilon)}, \quad l_3 = \rho \bar{y}, \quad u_3 = \bar{y}, \\
f_4(u, k, y; \rho, \epsilon) &:= -e^{ik \cdot \hat{y}(\rho \bar{y} + ui)}, \quad l_4 = -\epsilon, \quad u_4 = \epsilon,
\end{aligned} \tag{14}$$

where ρ is a small real positive parameter introduced for convenience. We will discuss the limit $\rho \rightarrow 0$ below. Occasionally, we will abbreviate $f(u, k, y; \rho, \epsilon)$ as $f(k, y)$.

We now define ten contour integrals I_i which all vanish by Eq.(13). We exploit the fact that a propagator $\Delta_F(x_1 - x_2)$ provides a vector $y = x_1 - x_2$, which can serve to define the parallel space which we want to complexify. By construction, our approach demands that the contour $\Gamma(y)$ runs in the complexified real space which is defined by a propagator which connects two vertices. The very presence of such a propagator allows the definition of the one-dimensional parallel space. So we cannot connect vertices at two arbitrarily chosen points x, y by a contour, but have to choose vertices which are connected by a propagator $\Delta_F(x - y)$.

All our contours Γ will have the property that they consists of two sub-paths $\gamma_{i,1}$ and $\gamma_{i,3}$, which run parallel to but above ($\text{Im}(z) > 0$) or below ($\text{Im}(z) < 0$) the real axis. We call them horizontal paths. The two other sub-paths $\gamma_{i,2}$ and $\gamma_{i,4}$ run parallel to the imaginary axis through the endpoints of the parallel paths.

If we want to stress the ρ dependence of various integrals I_i , we write $I_i(\rho)$. Occasionally, we will also consider the ρ dependence of individual integrals $I_{i,j}(\rho)$, where the second subscript refers to the enumeration of f_j in I_i .

We group the ten contour integrals in three classes. The first class provides I_1, I_5, I_6, I_{10} :

$$\begin{aligned}
0 = I_1 &:= \int \frac{d^4 k}{k^2} \frac{d^4 r}{r^2} \int dX G(x_a, x_b, x_c, x_d, x_0) \\
&\quad \times \Delta_F^5(x_r - x_l, x_b - x_l, x_m - x_a, x_d - x_r, x_r - x_c) \\
&\quad \times e^{ik \cdot (x_l - x_m)} e^{ir \cdot (x_0 - x_l)} \left[\sum_{i=1}^4 \int_{l_i}^{u_i} du f_i(-r, x_m - x_l) \right],
\end{aligned} \tag{15}$$

$$\begin{aligned}
0 = I_5 &:= - \int \frac{d^4 k}{k^2} \frac{d^4 r}{r^2} \int dX G(x_a, x_b, x_c, x_d, x_0) \\
&\quad \times \Delta_F^5(x_r - x_l, x_b - x_l, x_l - x_a, x_d - x_m, x_r - x_c) \\
&\quad \times e^{ik \cdot (x_m - x_r)} e^{ir \cdot (x_0 - x_r)} \left[\sum_{i=1}^4 \int_{l_i}^{u_i} du f_i(-r, x_m - x_r) \right],
\end{aligned} \tag{16}$$

$$\begin{aligned}
0 = I_6 &:= \int \frac{d^4 k}{k^2} \frac{d^4 r}{r^2} \int dX G(x_a, x_b, x_c, x_d, x_0) \\
&\quad \times \Delta_F^5(x_r - x_l, x_b - x_l, x_l - x_a, x_d - x_r, x_m - x_c) \\
&\quad \times e^{ik \cdot (x_r - x_m)} e^{ir \cdot (x_0 - x_r)} \left[\sum_{i=1}^4 \int_{l_i}^{u_i} du f_i(-r, x_m - x_r) \right],
\end{aligned} \tag{17}$$

$$\begin{aligned}
0 = I_{10} &:= - \int \frac{d^4 k}{k^2} \frac{d^4 r}{r^2} \int dX G(x_a, x_b, x_c, x_d, x_0) \\
&\quad \times \Delta_F^5(x_r - x_l, x_b - x_m, x_l - x_a, x_d - x_r, x_r - x_c)
\end{aligned} \tag{18}$$

$$\times e^{ik \cdot (x_m - x_l)} e^{ir \cdot (x_0 - x_l)} \left[\sum_{i=1}^4 \int_{l_i}^{u_i} du f_i(-r, x_m - x_l) \right],$$

where $\Delta_F^5(x_r - x_l, x_b - x_l, \dots, x_r - x_c)$ denotes the product of five propagators $\Delta_F(x_r - x_l) \Delta_F(x_b - x_l), \dots, \Delta_F(x_r - x_c)$. The signs in front of the definitions of I_5 and I_{10} are determined by the various orientations and will be explained below.

We mentioned already that the 4TR has a distinguished propagator, which has an endpoint x_m which couples at four different points in the four terms. Referring to Fig.(3), we call this point z when it moves along one of the four contour integrals above. Each of the four cases in this figure corresponds to one of the four terms in the 4TR, in the sense that the contours reproduce the Feynman integral when the integrand of the contour for f_2 is evaluated at $u = 0$. There, f_2 evaluates to $e^{iy \cdot k}$ (for generic y, k) and thus reproduces the propagator $\Delta_F(x_0 - x_m)$ upon inverse Fourier transformation. So, at $u = 0$, the function f_2 in I_1 reproduces the Feynman graph \mathcal{G}_1 , and similarly I_{10} matches \mathcal{G}_2 , I_6 matches \mathcal{G}_3 and I_5 matches \mathcal{G}_4 .

Note that when moving this endpoint along, there still remains a two-point vertex at the point x_m . Note further that our contours move the point z close to one of the endpoints of the propagator $\Delta_F(x_l - x_r)$; the point z will actually traverse one of these endpoints in the limit $\rho \rightarrow 0$ at the point $u = 0$ in f_4 .

The second class provides I_2, I_4, I_7, I_9 :

$$\begin{aligned} 0 = I_2 &:= \int \frac{d^4 k}{k^2} \frac{d^4 r}{r^2} \int dX G(x_a, x_b, x_c, x_d, x_0) \\ &\quad \times \Delta_F^5(x_r - x_l, x_0 - x_l, x_b - x_l, x_d - x_r, x_r - x_c) \\ &\quad \times e^{ir \cdot (x_l - x_a)} \left[\sum_{i=1}^4 \int_{l_i}^{u_i} du f_i(r - k, x_m - x_l) \right], \end{aligned} \quad (19)$$

$$\begin{aligned} 0 = I_4 &:= - \int \frac{d^4 k}{k^2} \frac{d^4 r}{r^2} \int dX G(x_a, x_b, x_c, x_d, x_0) \\ &\quad \times \Delta_F^5(x_r - x_l, x_0 - x_r, x_b - x_l, x_l - x_a, x_r - x_c) \\ &\quad \times e^{ir \cdot (x_d - x_r)} \left[\sum_{i=1}^4 \int_{l_i}^{u_i} du f_i(k - r, x_m - x_r) \right], \end{aligned} \quad (20)$$

$$\begin{aligned} 0 = I_7 &:= \int \frac{d^4 k}{k^2} \frac{d^4 r}{r^2} \int dX G(x_a, x_b, x_c, x_d, x_0) \\ &\quad \times \Delta_F^5(x_r - x_l, x_0 - x_r, x_b - x_l, x_l - x_a, x_d - x_r) \\ &\quad \times e^{ir \cdot (x_r - x_c)} \left[\sum_{i=1}^4 \int_{l_i}^{u_i} du f_i(r - k, x_m - x_r) \right], \end{aligned} \quad (21)$$

$$\begin{aligned} 0 = I_9 &:= - \int \frac{d^4 k}{k^2} \frac{d^4 r}{r^2} \int dX G(x_a, x_b, x_c, x_d, x_0) \\ &\quad \times \Delta_F^5(x_r - x_l, x_0 - x_l, x_l - x_a, x_d - x_r, x_r - x_c) \\ &\quad \times e^{ir \cdot (x_b - x_l)} \left[\sum_{i=1}^4 \int_{l_i}^{u_i} du f_i(k - r, x_m - x_l) \right]. \end{aligned} \quad (22)$$

This time, it is the two-point vertex at x_m itself which moves along a similar contour. It is the sole purpose of the contours in the second class to move this point close to x_l (on the “left”) or x_r (on the “right”). We need it there to make contact with the curves in the third class. As we move the whole two-point vertex, the functions f_i will depend on two momenta in the form $k - r$ or $r - k$. As long as $\rho \neq 0$, the point x_m will not merge with either x_l or x_r . This is in fact a very dangerous point. The moment when x_m collapses to one of these points, the total number of propagators in our Feynman diagram is reduced by one, and thus the powercounting can change drastically. Especially, it might and will in general happen that we generate subdivergences in the collapse. This is what really makes the 4TR a *four*-term relation. We will see that we can arrange only four contours in a manner so that the collapse at x_l or x_r always happens twice, with opposite signs. Hence, two contours stabilize the collapse at x_l and two further ones at x_r . These cancellations then allow for the limit $\rho \rightarrow 0$ at the end, and generate the 4TR with the promised signs.

The third class defines I_3, I_8 . It slightly modifies the f_i and only becomes a proper contour integral in the limit $\rho \rightarrow 0$:

$$\begin{aligned}
0 = \lim_{\rho \rightarrow 0} I_3 &:= - \int \frac{d^4 k}{k^2} \frac{d^4 r}{r^2} \frac{d^4 m}{m^2} \frac{d^4 m_1}{m_1^2} \frac{d^4 m_2}{m_2^2} \int dX G(x_a, x_b, x_c, x_d, x_0) \\
&\times \Delta_F(x_b - x_l) \Delta_F(x_r - x_c) \\
&\times e^{ik \cdot (x_r - x_l)} e^{im_1 \cdot (x_l - x_a)} e^{im_2 \cdot (x_d - x_r)} e^{ir \cdot (x_0 - x_l)} \\
&\times \left[\sum_{i=1}^4 \int_{l_i}^{u_i} du \tilde{f}_i(u, r, m_1, m_2, m, x_l - x_r; \rho, \epsilon) \right], \tag{23}
\end{aligned}$$

$$\begin{aligned}
0 = \lim_{\rho \rightarrow 0} I_8 &:= \int \frac{d^4 k}{k^2} \frac{d^4 r}{r^2} \frac{d^4 m}{m^2} \frac{d^4 m_1}{m_1^2} \frac{d^4 m_2}{m_2^2} \int dX G(x_a, x_b, x_c, x_d, x_0) \\
&\times \Delta_F(x_l - x_a) \Delta_F(x_d - x_r) \\
&\times e^{ik \cdot (x_r - x_l)} e^{im_1 \cdot (x_b - x_l)} e^{im_2 \cdot (x_r - x_c)} e^{ir \cdot (x_0 - x_l)} \\
&\times \left[\sum_{i=1}^4 \int_{l_i}^{u_i} du \tilde{f}_i(u, r, m_1, m_2, m, x_l - x_r; \rho, \epsilon) \right], \tag{24}
\end{aligned}$$

where \tilde{f} is defined below. These two contour integrals once more move the same distinguished propagator as the contours in the first class. In the limit $\rho \rightarrow 0$, all dependence on the location of the point x_m disappears. It is either collapsed to x_l or x_r .

Note that this time we explicitly gave five propagators in Fourier transformed form in Eq.(23,24). However, the total number of propagators that are not summarized in $G(x_a, x_b, x_c, x_d, x_0)$ is still seven, since two remain in coordinate form. This time we use the propagator $\Delta_F(x_l - x_r)$, present in all four terms, to define the parallel space and to connect the “left side” (x_a, x_b) with the “right side” (x_c, x_d) . For I_3 , this happens while x_m approaches the collapse either along the propagators $\Delta_F(x_l - x_a)$ or $\Delta_F(x_d - x_r)$, while for I_8 , x_m runs either along $\Delta_F(x_b - x_l)$ or $\Delta_F(x_c - x_r)$. Our orientations are such that all vertical paths which coincide in the limit $\rho \rightarrow 0$ have opposite orientations.

We note that in the limit $\rho \rightarrow 0$

$$\tilde{f}_i(u, r, m_1, m_2, m, x_l - x_r; \rho, \epsilon) = f_i(u, r, x_l - x_r; \rho, \epsilon), \quad \forall m_1, m_2, m, \quad (25)$$

according to the following definition of $\tilde{f}_i(u, r, m_1, m_2, m, x_l - x_r; \rho, \epsilon)$

$$\begin{aligned} 0 &< \rho \ll 1, \\ e_1 &:= x_m - x_l, \text{ for } I_3, \quad x_l - x_m, \text{ for } I_8, \\ e_2 &:= x_r - x_m, \text{ for } I_3, \quad x_m - x_r, \text{ for } I_8, \\ \tilde{f}_2(u, r, m_1, m_2, m, x_l - x_r; \rho, \epsilon) &:= f_2(u, r, x_l - x_r; 0, \epsilon) e^{i\rho(m_1+m) \cdot e_1}, \\ \tilde{f}_4(u, r, m_1, m_2, m, x_l - x_r; \rho, \epsilon) &:= f_4(u, r, x_l - x_r; 0, \epsilon) e^{i\rho(m_2+m) \cdot e_2}, \\ \tilde{f}_i(u, r, m_1, m_2, m, x_l - x_r; \rho, \epsilon) &:= f_i(u, r, x_l - x_r; 0, \epsilon) \quad \forall i \in \{1, 3\}. \end{aligned} \quad (26)$$

In the limit $\rho \rightarrow 0$ the m integration in I_3, I_8 as well as the k integration in $I_{2,4}, I_{4,4}, I_{7,4}$ and $I_{9,4}$ decouples. It is easy to see that such integrations are independent of the orientation of the vector $e = e_{1,2}$ defining the parallel space, due to rotational invariance of the measure $\int d^4m$:

$$\int d^4m \frac{e^{i\rho m \cdot e}}{m^2} \sim \int dm_{\parallel} \sqrt{m_{\parallel}^2} [e^{i\rho \bar{e} m_{\parallel}} + e^{-i\rho \bar{e} m_{\parallel}}], \quad \forall e, \quad (27)$$

We do not worry at this point that this integral is ill-defined. We use a cut-off λ and will later see that all these contributions vanish.

Note further that with these definitions the horizontal paths in class three cancel out:

$$I_{3,1} + I_{8,1} = I_{3,3} + I_{8,3} = 0, \quad (28)$$

by construction. For these horizontal paths, the f_i s remain ρ -independent, and thus Eq.(28) follows from using Eq.(12) backwards for the m_1, m_2 integrations.

We already stressed that the integrals $I_{1,2}, I_{5,2}, I_{6,2}, I_{10,2}$ contain the Feynman integrals \mathcal{G}_i at the point $u = 0$. They are in fact ill-defined at this point if we let the cut-off in the final $\int d^4k$ integration go to infinity. It is our main purpose to show that the only remaining contributions which diverge for large cut-off come from these $I_{i,2}$. Thus, what has to be shown is that neither the horizontal paths diverge at the end, nor the vertical paths apart from the ones in Eq.(7). Not unexpectedly, the horizontal paths will become finite when one considers the paths above and below the real axis together, and the vertical paths cancel in appropriate pairs (or quartets) due to their opposite orientations.

To this end, we show that the following four propositions hold.

Proposition 1 *For $i \in \{1, 2, 4, 5, 6, 7, 9, 10\}$ we have*

$$< I_{i,1}(\rho) + I_{i,3}(\rho) > = 0, \quad \forall \rho > 0. \quad (29)$$

Proof: For our horizontal paths, the endpoints of the u -integrations depend on coordinates x_l, x_r, x_m . We thus cannot interchange the u -integration with these integrations. Accordingly, we will do the u -integration first.

But we can integrate last the momentum which appears in the f -function. Let us call this momentum k . For this momentum integration, we will use the measure $\int d^4k$ separated in parallel and orthogonal space integrations.

First, integrating u delivers

$$\int_{\rho\bar{y}}^{\bar{y}} du e^{iuk_{\parallel}} = \frac{e^{iy \cdot k} - e^{iy \cdot \rho k}}{ik_{\parallel}}, \quad (30)$$

where k_{\parallel} is the component of the four-momentum k in the direction of the four-vector y , which is one of the differences of coordinates as they appear in the functions f_1, f_3 in the integrals in the proposition. After the u integration, we will do all remaining integrals but the k integration. Inspection of Eqs.(30) and (15-18,23,24) shows that the integrand is a proper Feynman integral concerning these integrations, with k or ρk acting as an exterior momentum for these integrations.

Doing all integrations but the k integration, we know from powercounting that there remains a factor d^4k/k^4 , expressing the overall logarithmic divergence. Thus, the results of all but the last integration is to multiply Eq.(30) by $c(\rho)d^4k/k^4$, where $c(\rho)$ is a pure number obtained from finite integrations over coordinates and momenta.

For the practitioner of computational field theory, the calculation of the penultimate integration is the end of the story. The finite value so obtained ($c(\rho)$ in our case) determines the coefficient of the divergence in the final momentum integration. The divergence would be provided by a behaviour $\sim \log(\lambda)$ if we use a cut-off λ in the final integration, for a logarithmic divergent Feynman integral. What for us remains to do is to check if the final momentum integration provides a divergence along the horizontal paths.

From the u -integration of Eq.(30) and the overall factor of $c(\rho)d^4k/k^4$, we find that the paired horizontal paths deliver

$$c(\rho) \int_{-\lambda}^{\lambda} dk_{\parallel} \int d^3k_{\perp} \left[\frac{e^{-\epsilon k_{\parallel}} - e^{\epsilon k_{\parallel}}}{k_{\parallel}} \right] \frac{1}{[k^2]^2} \sim c(\rho) \int_{-\lambda}^{\lambda} dk_{\parallel} \left[\frac{e^{-\epsilon k_{\parallel}} - e^{\epsilon k_{\parallel}}}{k_{\parallel}} \right] \frac{1}{\sqrt{k_{\parallel}^2}} \quad (31)$$

where $k^2 = k_{\parallel}^2 + k_{\perp}^2$, and the exponentials resulted from the appearance of ϵ in Eq.(14).⁹ We stress that in the final k_{\parallel} integration we are only interested in the (UV-) behaviour for large k_{\parallel} . The behaviour near $k_{\parallel} = 0$ is of no interest for us. Accordingly, we nullified all external parameters. This has not changed the UV behaviour at all, but for the behaviour near $k_{\parallel} = 0$ we should have in mind that the IR behaviour is in fact dependent on the value of external parameters like masses and momenta.¹⁰ The pole at $k_{\parallel} = 0$ is in fact fictitious and absent if we keep a mass or momentum $\neq 0$. Equivalently, from now on it is implicitly understood that we use a small IR cut-off in the final k_{\parallel} integration.

It may appear odd that the final momentum integration involves a non-covariant separation between k_{\parallel} and k_{\perp} . To see how this may arise, consider the following

⁹We work in Euclidean space for convenience. It is possible to work in Minkowski space as well. One merely has to show that for k_{\parallel} timelike or spacelike similar expressions result.

¹⁰In dimensional regularization, we would simply keep a scale in the final momentum integration.

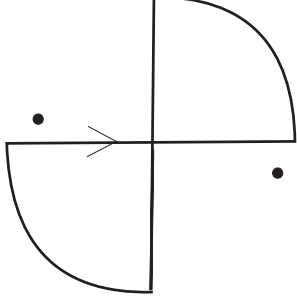


Figure 5: The contour rotation. The two dots indicate the endpoints of the cuts from $(k_{\parallel}^2 + i\sigma)^{1/2}$.

integral

$$\begin{aligned} & \int d^4x \int d^4k \int du F(k^2, x^2, k \cdot x, u) \\ &= \int d\Omega_{\hat{x}} \int d^4k \int du \int d\bar{x} \bar{x}^3 F(k^2, x^2, k \cdot x, u) \end{aligned} \quad (32)$$

$$= \int d\Omega_{\hat{x}} \int d^4k \int du G(k^2, k \cdot \hat{x}, u) \quad (33)$$

$$= 2\pi^2 \int d^4k \int du G(k^2, k_{\parallel}, u). \quad (34)$$

After all but two of the integrations have been performed, one obtains a covariant integral over a coordinate x and momentum k and a contour variable u , whose integrand F can depend only on the three scalar products and u . In Eq.(32) we perform first the integral over $\bar{x} := \sqrt{x^2}$. In Eq.(33) the result of the \bar{x} integration must yield a function G that depends only on k^2 , the component of k in the direction of the unit vector \hat{x} and u . Since the d^4k integration can leave no dependence on the direction of \hat{x} , in Eq.(34) we may replace the angular integration by the value, $2\pi^2$, of the surface of the unit-sphere in four dimensions, and also replace $k \cdot \hat{x}$ by k_{\parallel} which is a component of k along *any* fixed axis.

By construction, $c(\rho)$ is a finite quantity for all $\rho \neq 0$. What remains to prove the theorem is to show that the integral in Eq.(31) remains finite for large λ .

We proceed with the k_{\parallel} integration. Due to the factor $[e^{-\epsilon k_{\parallel}} - e^{\epsilon k_{\parallel}}]/k_{\parallel}$ this is not a standard loop integration. We achieve the k_{\parallel} integration, which is along the real axis, by analytic continuation to the imaginary axis in complex k_{\parallel} space. The integration $\int_{-\lambda}^{\lambda} dk_{\parallel}$ becomes a closed contour by adding an arc with radius λ from $+\lambda$ to $+i\lambda$ (counterclockwise!), integrating along the imaginary axis from $+i\lambda$ to $-i\lambda$ and another arc from $-i\lambda$ to $-\lambda$ (clockwise). We read $\sqrt{k_{\parallel}^2}$ above as $\sqrt{k_{\parallel}^2 + i\sigma}$, $0 < \sigma \ll 1$, as this does not change the value of the integral. Then the integrand remains single-valued along and inside the contour in Fig.(5).

We conclude that the integration from $-\lambda$ to λ is given by the three terms above. We show next that the two arcs add to a finite contribution. With $z = \lambda e^{i\phi}$ we

obtain

$$\frac{i}{\lambda} \int_0^{\pi/2} d\phi \left[e^{\lambda e^{i\phi}} e^{-i\phi} - e^{-\lambda e^{i\phi}} e^{-i\phi} \right] - \frac{i}{\lambda} \int_{\pi}^{3\pi/2} d\phi \left[e^{\lambda e^{i\phi}} e^{-i\phi} - e^{-\lambda e^{i\phi}} e^{-i\phi} \right], \quad (35)$$

which adds to zero upon setting $\phi' = \phi - \pi$ in the second integration.

One readily verifies that the integration along the imaginary axis is finite. It provides an expression

$$ic(\rho) \int_0^\lambda dk_{\parallel} \left[\frac{e^{-i\epsilon k_{\parallel}} - e^{i\epsilon k_{\parallel}}}{k_{\parallel}} \right] \frac{1}{\sqrt{k_{\parallel}^2}} < \infty. \quad (36)$$

This completes the proof. \square

This proposition guarantees that for $\rho > 0$ the horizontal paths in the proposition are well defined when our momentum integrations tend to infinity. Further, it follows that $\langle I_{j,2} + I_{j,4} \rangle = 0$, $\forall j \in \{2, 4, 7, 9\}$, $\forall \rho > 0$.

Next, we can prove the following proposition.

Proposition 2 *We have*

$$\langle I_{1,4} + I_{3,2} \rangle = \langle I_{5,4} + I_{3,4} \rangle = \langle I_{6,4} + I_{8,4} \rangle = \langle I_{10,4} + I_{8,2} \rangle = 0, \quad \forall \rho > 0. \quad (37)$$

Proof: The proposition compares integrals of the first class with integrals of the third class in pairs. In these pairs, the elements of the first class are distinguished from elements of the third class by two facts: they use different propagators to define the parallel space, and the point x_m is at different locations.

But the point x_m is only a two-point vertex. From our experience with integrals in the second class we know that we can transport it freely as long as it does not collapse to either x_l or x_r .

Hence, for all integrals $I_{i,4}$ in the first class we use contour integrals as provided by the second class to transport the point x_m . We move it so that it is in the same position as in the integrals of the third class in the proposition.

Next, we assume that we carried out all $\int dX$ integrations. The remaining integrations concern $\int du$ and momentum integrations.¹¹ We now proceed by the following argument. A diagram which is free of subdivergences can be opened at any line, its value is independent from the point where we cut the diagram. The finite value assigned to the diagram after the penultimate integration appears as the coefficient of divergence in the final loop integration and is uniquely determined after the penultimate integration is carried out. It is only the final integration which diverges (in subdivergence free diagrams).

Now, we cut the diagram at the propagator which involves the factor $e^{-u\epsilon r_{\parallel}}$. This has the advantage that the remaining expression is u -independent. All u dependence affects only the final loop integration. Such a propagator always exist,

¹¹Here, we use that the u integration is decoupled from the integration of the coordinates for vertical paths. We further exchange orders of integrations at will, which is legitimate for any $\lambda < \infty$ and $\rho > 0$, where our Feynman integrands are fairly well-defined analytic functions.

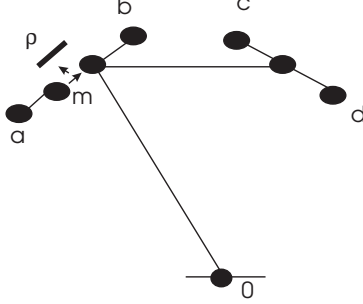


Figure 6: The appearance of a subdivergence at $\rho = 0$.

by inspection of Eqs.(15-18) and of Eqs.(19-22). As a consequence, only the final momentum integration depends on the variable u , and will be of the general form

$$\int_{-1}^1 du \int d^4 r \frac{c e^{-\epsilon u r_{\parallel}}}{[r^2]^2}, \quad (38)$$

as our overall degree of divergence was logarithmic. Here, c is the uniquely determined u -independent value of the diagram after all momentum integrations but the final one are carried out. The u integration runs in this parametrization from $\int_{-1}^1 du$ for vertical paths from below to above the real axis, and vice versa for vertical paths with the opposite orientation.

But the vertical contours which are paired in the proposition have opposite orientation, but otherwise their integrands must agree after the penultimate integration. This proves the proposition.¹² \square

Our next proposition involves the limit $\rho \rightarrow 0$. The main obstacle in this limit is that subdivergences may appear. In this limit, we effectively decoupled a propagator. The weight of this propagator is thus missing in the powercounting for the remainder. This, in general, will generate a subdivergence. We will see that with our choice of orientations the relevant combinations of contours still allow the limit $\rho \rightarrow 0$. In Fig.(6) we demonstrate the presence of the subdivergence at $\rho = 0$. Figs.(7,8,9) demonstrate the various orientations of the contours.

We collect all combinations of contributions which have to cancel for $\rho \rightarrow 0$ in a proposition.

Proposition 3 *In the limit of $\rho \rightarrow 0$ we have*

$$\begin{aligned} \langle I_{1,1} + I_{1,3} + I_{10,1} + I_{10,3} \rangle &= 0 \quad (Ia), \\ \langle I_{5,1} + I_{5,3} + I_{6,1} + I_{6,3} \rangle &= 0 \quad (Ib), \\ \langle I_{2,1} + I_{2,3} + I_{9,1} + I_{9,3} \rangle &= 0 \quad (IIa), \end{aligned}$$

¹²A different proof may be obtained by isolating the singularity at $u = 0$ in appropriate functions f_2 or f_4 . At these points, the paired integrands match and cancel out. Isolating the singularities is most easily obtained by replacing the complex plane by \mathbf{R}^2 , with $u \rightarrow iu$, which effectively introduces rapidly oscillating integrands whenever $u \neq 0$ in vertical paths.

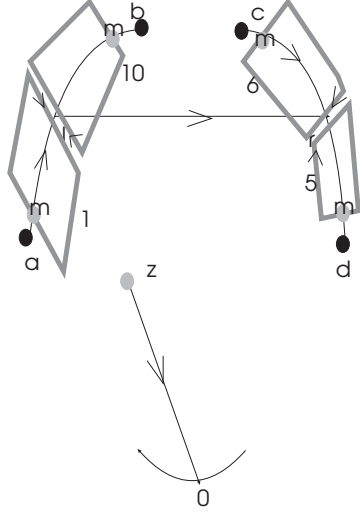


Figure 7: The orientations for the first class I_1, I_5, I_6, I_{10} . Orientations are chosen in accordance with Eq.(14) and Eqs.(15-24) such that the various propositions hold. For class 1 all contours are oriented clockwise; the grey dots denote the point x_m in each contour. The point z moves along the contours. At $z = x_m$ we recover a genuine Feynman graph. The contours will cross the points x_l or x_r if $\rho = 0$.

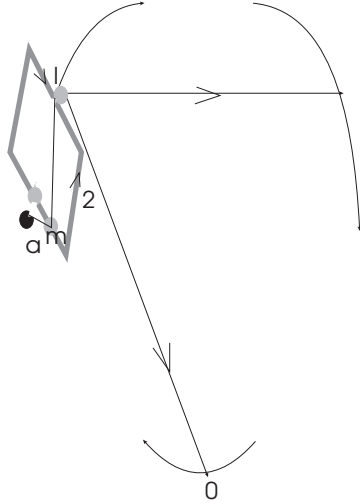


Figure 8: I_2 as an example for the second class. I_4, I_7, I_9 are similar and located in the same places as their partners from the first class in Fig.(7). By comparison with the previous figure, we realize that it is now the former x_m which moves. For $\rho = 0$, the contour traverses x_l .

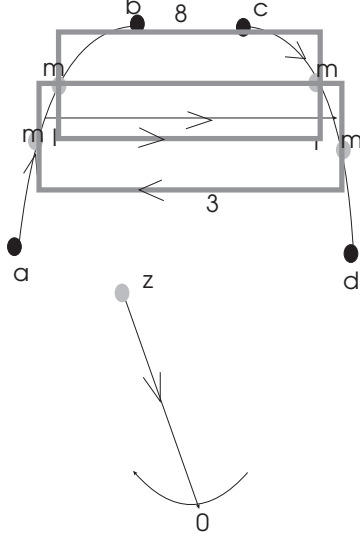


Figure 9: The two grey rectangles indicate the two contours I_3, I_8 . They coincide and cancel at $\rho = 0$. The point x_m moves from the left to the right as long as $\rho \neq 0$, but disappears at $\rho = 0$.

$$\begin{aligned}
 < I_{7,1} + I_{7,3} + I_{4,1} + I_{4,3} > &= 0 \quad (IIb), \\
 < I_{1,4} + I_{3,2} + I_{10,4} + I_{8,2} > &= 0 \quad (IIIa), \\
 < I_{5,4} + I_{3,4} + I_{6,4} + I_{8,4} > &= 0 \quad (IIIb).
 \end{aligned}$$

Proof: Following our general philosophy, we assume that all momentum integrations are cut-off by an appropriate λ . Then, all analytic expressions are well-defined $\forall \rho$ and have a finite limit when ρ tends to zero. We thus only have to check that the above proposition combines integrals such that they approach the same limit when $\rho \rightarrow 0$, but with opposite orientations, so that they identically cancel, cf. Figs.(7,8,9). We then let $\lambda \rightarrow \infty$ afterwards.

For (Ia), we note that $I_{1,1} + I_{1,3}$ is well defined for all ϵ , as well as $I_{10,1} + I_{10,3}$, and for all $\rho \neq 0$, by Prop.(1). At $\rho = 0$, the two pairs approach the same limit, by inspecting Eqs.(15-18). But at $\rho = 0$, the integrands of the two pairs equal and the contours are oriented in the opposite manner. Thus they cancel identically. Similar arguments hold for case (Ib).

For (IIa,IIb) again a similar argument holds, inspecting Eqs.(19-22).

For cases (IIIa) and (IIIb) once more, the given combinations of integrals exist for any $\rho > 0$ and cancel out at $\rho = 0$. To see this, one simply considers Eqs.(15-18) and (23,24) and checks the definitions of \tilde{f}_i in Eqs.(26) and various orientations in Figs.(7,9). In fact, \tilde{f} was defined such that its vertical paths f_4 in the second class agree with the oppositely oriented vertical paths in the third class. \square

Summarizing our considerations, we recover Eq.(6)

$$\begin{aligned}
0 &= \left\langle \sum_{i=1}^{10} I_i \right\rangle \\
&= \left\langle I_{1,2} + I_{5,2} + I_{6,2} + I_{10,2} \right\rangle .
\end{aligned} \tag{39}$$

To prove the theorem, it remains to show that these four terms deliver the overall divergences of \mathcal{G}_i , with the correct signs.

First of all, we check that the remaining contributions give the integrals we want. With $\Lambda := \int_1^\lambda dt e^{\epsilon t}/t^2$, we claim that the following proposition holds.

Proposition 4

$$\lim_{\lambda \rightarrow \infty} I_{i,2}/\Lambda =: \langle I_{i,2} \rangle \sim \langle \mathcal{G}_r \rangle =: \lim_{\lambda \rightarrow \infty} \mathcal{G}_r / \log(\lambda) < \infty, \tag{40}$$

where the i and r indices match as in Eq.(7), and where our propositions demand that we use the same ϵ for all i .

Proof: First note that the four $I_{i,2}$ are ρ -independent. They all appear at the endpoints $u = y$ in vertical paths f_2 .

We once more cut at the r -integration, cf. Eq.(15-18), again exploiting that all u dependence is in the final integration. It is of the form

$$\begin{aligned}
\lim_{\lambda \rightarrow \infty} I_{i,2} &\sim \lim_{\lambda \rightarrow \infty} \int_{-\lambda}^{\lambda} dr_{\parallel} \int d^3 r_{\perp} \int_{-\epsilon}^{\epsilon} du \frac{ce^{-ur_{\parallel}}}{[r_{\parallel}^2 + r_{\perp}^2]^2} \\
&\sim \lim_{\lambda \rightarrow \infty} \int_{-\lambda}^{\lambda} dr_{\parallel} \frac{c[e^{\epsilon r_{\parallel}} - e^{-\epsilon r_{\parallel}}]}{r_{\parallel} \sqrt{r_{\parallel}^2}} \sim \lim_{\lambda \rightarrow \infty} \int_1^{\lambda} dr_{\parallel} \frac{ce^{\epsilon r_{\parallel}}}{r_{\parallel}^2} = c \lim_{\lambda \rightarrow \infty} \Lambda, \tag{41}
\end{aligned}$$

$$\mathcal{G}_r \sim \lim_{\lambda \rightarrow \infty} \int_1^{\lambda} dr_{\parallel} \frac{c}{r_{\parallel}} \sim c \log(\lambda), \tag{42}$$

where c is the actual ϵ -independent coefficient of the overall divergence we are interested in, and which appears after the penultimate momentum integration is carried out. We restricted ourselves to terms which diverge for large cut-off λ . This justified that we abandoned terms involving $e^{-\epsilon r_{\parallel}}$, and that we deliberately cut off the final r_{\parallel} integration at the lower boundary at 1. Eqs.(41) and (42) show that the vanishing of $\langle I_{i,2} \rangle$ is equivalent to the vanishing of the appropriate matched $\langle \mathcal{G}_r \rangle$. Further, with the orientations of the various contours chosen as demanded by the previous propositions, the signs are as in Eq.(7). \square

The attentive reader may have asked her/himself whether the arguments of Prop.(1) could be extended to prove that each term in the four-term relation is separately finite, thereby making Prop.(4) trivial. As an aside, we here indicate the analytical obstruction that fortunately prevents such a trivialization.

We have to integrate u from $-\epsilon$ to ϵ . At $u = 0$ we encounter the proper Feynman integral which will not allow for the limit $\lambda \rightarrow \infty$. It is easy to see that for $u \neq 0$ we could analytic continue r_{\parallel} to the imaginary axis, so that these contributions

($|u| \in [\eta, \epsilon]$, $0 < \eta < \epsilon$) remain finite for large cut-off, as we get rapidly oscillating integrands for large final loop momentum.

Let us now investigate the behaviour near $u = 0$. We once more insert a small imaginary part $i\sigma$ in the propagators, which will not alter the value of the integral along the real axis, but guarantees the absence of poles (or cuts) in the analytic continuation. In terms of the rescaled four-momentum $p = \eta r$ we investigate the behaviour as $\eta \rightarrow 0$ of an expression of the form

$$\begin{aligned}
& \int_{-\lambda}^{\lambda} dr_{\parallel} \int_0^{\infty} r_{\perp}^2 dr_{\perp} \int_{-\eta}^{\eta} du \frac{e^{-ur_{\parallel}}}{[r_{\parallel}^2 + r_{\perp}^2 + i\sigma]^2} \\
&= \int_{-\lambda}^{\lambda} dr_{\parallel} \int_0^{\infty} r_{\perp}^2 dr_{\perp} \frac{e^{\eta r_{\parallel}} - e^{-\eta r_{\parallel}}}{r_{\parallel}[r_{\parallel}^2 + r_{\perp}^2 + i\sigma]^2} \\
&= \eta \int_{-\lambda\eta}^{\lambda\eta} dp_{\parallel} \int_0^{\infty} p_{\perp}^2 dp_{\perp} \frac{e^{p_{\parallel}} - e^{-p_{\parallel}}}{p_{\parallel}[p_{\parallel}^2 + p_{\perp}^2 + i\eta^2\sigma]^2}. \tag{43}
\end{aligned}$$

The last line above show that if we want to continue this so that we go from $e^{p_{\parallel}}$ to the oscillatory $e^{ip_{\parallel}}$ we confront a pinch singularity at $\eta = 0$. If we rotated the contour to imaginary p_{\perp} we would pick up principal values at $(ip_{\parallel})^2 = p_{\perp}^2$.

Having concluded the aside, we summarize the derivation of the four-term relation Eq.(4) as follows.

1. Eq.(6) used contour integration to show that the sum of 40 integrals necessarily vanishes.
2. Of these 40, only 4 remain after applying the conclusions of Props.(1-3).
3. Prop.(1) eliminates the 16 horizontal contributions of the first two classes. The 4 horizontal contributions from the third class cancel each other in Eq.(28), by definition.
4. Prop.(2) guarantees that the vertical contributions of the third class cancel the vertical contributions $I_{i,4}$, $i \in \{1, 5, 6, 10\}$ of the first class.
5. Prop.(3) guarantees that, even in the limit $\rho \rightarrow 0$, 6 of the 12 cancellations of Props.(1,2) remain valid. These 6 are sufficient to derive the 4TR.
6. Prop.(4) identifies the divergences of the 4 remaining integrals with the 4 counterterms.
7. The remarks following Prop.(4) remind us of the nontriviality of Eq.(6), which asserts the finiteness of a very specific combination of 4 divergent integrals.

Now let us explain our provisos *iii*) and *iv*) in the theorem. These constraints are to be considered as sufficient conditions. We will try to formulate necessary conditions in future work.

For the proof of Prop.(3) we had to show that in the limit $\rho \rightarrow 0$ pairs or quartets of integrals $I_{i,j}$ cancel each other. In this limit, there is always a propagator which decouples, cf. Fig(6). Implicitly, we assumed so far that this is a scalar propagator.

It provides for any finite λ a constant factor, multiplying the remaining expression, similar to Eq.(27).

This decoupling was the reason for the possible existence of a subdivergence. Now, this decoupled propagator appears actually at different places. It appears between the vertex at x_l , and vertices at x_a or x_b in the cases $I_2, I_{3,2}$ (for x_a) or $I_9, I_{8,2}$ (for x_b); or it appears between the vertex at x_r and vertices at x_c or x_d in the cases $I_4, I_{3,4}$ (for x_d) or $I_7, I_{8,4}$ (for x_c).

It may happen that this propagator $\Delta_F(s)$ is matrix valued, as it might carry spin-, Lorentz- and/or other indices, while the vertices V_l and V_r at x_l or x_r might carry indices as well.

For the contributions to cancel out as demanded in the proof of proposition (3) we need that

$$[V_i, \Delta_F(s)] = 0, \quad i \in \{l, r\}, \quad \forall s^2 > 0. \quad (44)$$

This explains condition *iii*) in the theorem. An example in case is when Δ_F is fermionic, and the V_i provide vector couplings. We then have that $[\not{k}, \gamma_\mu] \neq 0$, and thus expect the theorem to fail, due to contributions from UV subdivergences at $\rho = 0$. For example, $I_{j,2}$, $j \in \{3, 8\}$ confronts us with

$$\int d^4k \frac{\not{k} e^{-u\epsilon k_\parallel}}{k^4} = A_{\hat{s}} \Rightarrow A \sim 2 \int_0^\lambda dk_\parallel (e^{-u\epsilon k_\parallel} - e^{u\epsilon k_\parallel}), \quad (45)$$

where \hat{s} defines the exterior axis which defines k_\parallel , so that we obtain as the quantity measuring the failure of the 4TR

$$[\not{s}, \gamma_\mu] A. \quad (46)$$

Integrating u , the remaining expression for A is finite in the limit $\rho \rightarrow 0$, which entails $s^2 \rightarrow 0$. It thus spoils Prop.(3), as A is a coefficient of logarithmic divergence. A more detailed analysis of the general role of subdivergences will be given in future work.

For condition *iv*), we note that the presence of spin structures as

$$\frac{\not{k} \gamma_\mu \not{k}}{k^4} = -\frac{\gamma_\mu}{k^2} + 2 \frac{k_\mu \not{k}}{k^4}. \quad (47)$$

may make the theorem to fail. In such a case, one notes that in the limit $s^2 \rightarrow 0$, the demanded cancellations appear in the form $e^{ik \cdot s} - 1$, where now k refers to the final momentum integration for the subdivergence. If these factors are accompanied by scalar integrals, all our arguments go through. If they are accompanied by tensors of first degree (which are odd in k), we are safe as this effectively projects to the odd part of $e^{ik \cdot s}$, which vanishes at $s^2 = 0$.

But for tensors of second degree, we are in trouble. So, while the first term on the rhs of Eq.(47) behaves effectively as a scalar particle the second term is problematic. In $e^{ik \cdot s} - 1$, the term with the exp-function allows for a form-factor expansion

$$\sim Ag_{\mu\nu} + B\hat{s}_\mu \hat{s}_\nu, \quad (48)$$

due to the presence of \hat{s} in $e^{ik \cdot s}$, which defines a parallel space in the subdivergent diagram. The second term without the exp-function only allows for

$$\sim Ag_{\mu\nu}. \quad (49)$$

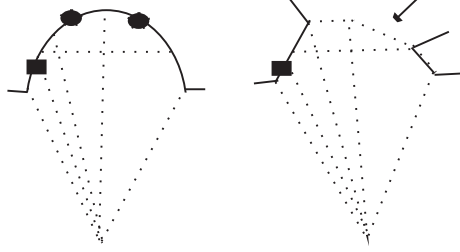


Figure 10: Two Feynman diagrams which result in the same analytic expression for nullified external momenta. We expect the one on the lhs to fulfil the 4TR, while the one on the rhs fail should fail.

Especially such a situation occurs when a propagator $x_m - x_l$ (or $x_m - x_r$) is part of a subdivergence only for one of the two cases which appear paired in proposition (3,(IIIa,b)). An example is when $I_{3,2}$ provides a subdivergence at $s^2 \neq 0$, while $I_{8,2}$ does only so at $s^2 = 0$.

This asymmetry provides us finally with an extra contribution which diverges with λ , which can be shown to have the form of a finite part of a two-loop integral of master topology [15]. A more detailed analysis will be given elsewhere.

4 A curious case study

If one wants to find explicit examples for the 4TR in action, one quickly realizes that there are not many at low loop numbers [15]; for graphs free of subdivergences. Either the examples at hand are trivial due to symmetries in the graph, or are very hard to calculate.

In such circumstances, one might wonder if it is possible to enlarge the number of available examples by allowing for nonrenormalizable couplings in the universal function $G(x_a, x_b, x_c, x_d, x_0)$, as this function will not directly affect the 4TR. In this section, we report on one such example, where the 4TR is bound to fail as the graphs considered violate one of our provisos. But we see that in this special case there is a way out, and the techniques used in this paper extend to manage this case and predict the results we are interested in. In the course of our consideration, we will learn that the problem we consider actually is directly sensitive to the before-mentioned UV-divergence which appears when one of the propagators decouples. The problem discussed here is calculated in [15], where the reader will find details of the calculation and a confirmation of the relation proposed here.

So we start with an interesting case where our 4TR will fail in its unmodified form. As envisaged, it is given when one allows for non-renormalizable couplings in the universal function $G(x_a, \dots, x_0)$, which violates proviso v).

Consider Fig.(10). It shows two Feynman diagrams. The first one contributes to a correction of a $\bar{\psi}\psi\phi^2$ coupling, say (it is as well a contribution to $\bar{\psi}\psi\phi^3$, by making the Yukawa coupling at the top into a $\bar{\psi}\psi\phi^2$ coupling with a zero-momentum

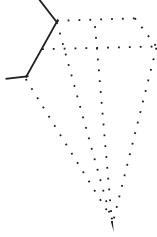


Figure 11: Shrinking the propagator $\Delta_F(x_m - x_l)$ of Fig.(10) to a point results in a five-loop graph with a four-loop subdivergence given in this figure.

external boson), while the other one contributes to $(\bar{\psi}\psi)^2$, for example. For the graph on the lhs external bosons couple with zero momentum at the two black blobs, which effectively bosonizes the two fermion fields as the coupling is of Yukawa type, with $(1/\not{k})\mathbf{1}(1/\not{k}) = 1/k^2$. Thus, for fermions with vanishing external momentum, both graphs result in the same analytic expression.¹³

Now we are in a very interesting situation: the analytic expression we have written down refers to two different Feynman graphs, and hence could refer to any linear combination of them. For the graph on the lhs all steps in our proof of the 4TR go through, while for the graph on the rhs they do not. If we transport the rectangle which corresponds to the endpoint z of the propagator $\Delta_F(x_0 - z)$ along the horizontal propagator to the other three endpoints demanded by the 4TR, it is clear that the graph on the rhs is in trouble: the horizontal propagator couples to two internal fermions on the left, while it couples to one internal fermion and one internal boson on the right. The four terms for the graph on the rhs thus obey different powercounting amongst them. Or, from the viewpoint of proviso *iii*), we have a situation $\Delta_{F,1}(s) - \Delta_{F,2}(s) \neq 0$, where we note that the two vertex factors are the same (they provide pure numbers, coupling constants) but the propagators for $x_r - x_c$, $(\Delta_{F,1}(s))$, and $x_d - x_r$, $(\Delta_{F,2}(s))$, are different. The arrow in Fig.(10) denotes the point where our 4TR will fail. In our notation, it is the graph \mathcal{G}_3 .

Now let us investigate what happens at the subdivergence, which appears when the propagator for $x_r - x_m$ shrinks to a point, and whose presence we believe to be the sole source of trouble for the graph on the rhs of Fig.(10). The corresponding Feynman graph for this subdivergence is given in Fig.(11).

We now consider solely the graphs which appear when the rectangular blob in Fig.(10) is located on the “right” in the graph on the lhs in the figure (in the figure, we explicitly give it only in the “left” \mathcal{G}_1 position). Then, it sits in the \mathcal{G}_3 or \mathcal{G}_4 position.

According to our previous analysis, we expect

$$0 = < I_4 + I_5 + I_{3,4} + I_{8,4} > . \quad (50)$$

¹³Once we have written down a theory involving Yukawa couplings and non-renormalizable ϕ -selfcouplings, the other couplings in both graphs like $\bar{\psi}\psi\phi^2$ and $(\bar{\psi}\psi)^2$ will be dynamically generated. This is important. When we restrict ourselves to renormalizable ϕ^4 selfcouplings, we will not generate any of the non-renormalizable coupling needed to generate the degeneracy of Feynman graphs coinciding with the same analytic expression.

Again collecting the remaining divergent contributions, and using the parts of Props.(1,2,3,4) which are still valid, we obtain

$$0 = \langle I_{3,4} + I_{5,2} + I_{6,2} + I_{8,4} \rangle. \quad (51)$$

Following our reasoning, this should be finite in the limit $\rho \rightarrow 0$ but the presence of the subdivergence.

For $\rho \neq 0$, actually only $I_{3,4}$ involves a subdivergence, due to the presence of the two-point vertex between x_r and x_c in $I_{8,4}$. Thus, the divergent behaviour of $\langle I_{5,2} + I_{6,2} \rangle$, we claim, is isolated in the subdivergence in $I_{3,4}$:

$$\langle I_{5,2} + I_{6,2} + I_{3,4} \rangle = 0. \quad (52)$$

So, we only have to consider the limit

$$\lim_{\rho \rightarrow 0} I_{3,4}. \quad (53)$$

We note that at $u = 0$ in f_4 the integrand for $I_{3,4}$ equals a Feynman integral which is identical with \mathcal{G}_4 .¹⁴ Integrating the convergent one-loop integral first, and then taking the limit $\rho \rightarrow 0$, one confirms that $\langle I_{3,4} \rangle = \langle I_{5,2} \rangle$. According to Prop.(1) horizontal paths should cancel, and thus $I_{5,2} = -I_{5,4} \Rightarrow I_{5,4} + I_{3,4} = 0$, in agreement with Prop.(2).

Collecting everything, we end up with the following expectation:

$$\langle \mathcal{G}_3 - 2\mathcal{G}_4 \rangle = 0. \quad (54)$$

In [15] we will report on a calculation confirming these expectations.

5 Conclusions

This finishes our consideration for the moment. We hope that these results shed some light on the connection between knot theory and UV divergences in a perturbative quantum field theory.

We also expect that the 4TR might be of practical value in future calculations, and hope that the close relation of UV divergences to weight systems, which comes quite unexpectedly, stimulates field theory, knot theory as well as number theory, where the question of classification of multiple zeta values (MZVs) [18] remains one of the most fascinating topics.

Also, relation Eq.(52) bears some resemblance with the STU relation, and deserves further study.

Acknowledgements

Ever since I started working on knots and renormalization I profitted much from David Broadhurst's enthusiasm and support. I also very much like to thank David

¹⁴This was first observed by D.J.Broadhurst.

Broadhurst for concerned and detailed reading and corrections of a preliminary version of the manuscript.

I thank Bob Delbourgo for generous and encouraging advice and for hospitality during a stay at the University of Tasmania, where some of these ideas came to mind. With equal pleasure I thank Peter Jarvis and Ioannis Tsohantjis for their stimulating interest in the subject.

References

- [1] D. Kreimer, Habilitationsschrift: *Renormalization and Knot Theory*, q-alg/9607022, J.Knot Th.Ram.**6**,4 (1997) 479-581.
- [2] D. Kreimer, Phys. Lett. **B354** (1995) 117.
- [3] D.J. Broadhurst and D. Kreimer, Int. J. Mod. Phys. **C6** (1995) 519.
- [4] D.J. Broadhurst, R. Delbourgo and D. Kreimer, Phys. Lett. **B366** (1996) 421.
- [5] D.J. Broadhurst, J.A. Gracey and D. Kreimer, Z.Phys.**C75** (1997) 559.
- [6] R. Delbourgo, A. Kalloniatis and G. P. Thompson, Phys. Rev. **D54** (1996) 5373; R. Delbourgo, D. Elliott, D.S. McAnally, Phys. Rev. **D55** (1997) 5230.
- [7] D.J. Broadhurst and A.V. Kotikov, *Compact analytical form for non-zeta terms in critical exponents at order $1/N^3$* , Open University preprint OUT-4102-67 (November 1996), hep-th/9612013.
- [8] D. Kreimer, *On Knots in subdivergent diagrams*, hep-th/9610128, to appear in Z.Phys.**C**.
- [9] D.J. Broadhurst and D. Kreimer, hep-th/9609128, Phys. Lett. **B393** (1997) 403.
- [10] D.J. Broadhurst, hep-th/9604128, to appear in J. Math. Phys.
- [11] J. M. Borwein and R. Girgensohn, Electronic J. Combinatorics **3** (1996) R23, with an appendix by D. J. Broadhurst.
- [12] J.M. Borwein, D.A. Bradley and D.J. Broadhurst, hep-th/9611004, Electronic J. Combinatorics **4** (1997) R5.
- [13] D.J. Broadhurst, *Conjectured Enumeration of irreducible Multiple Zeta Values, from Knots and Feynman Diagrams*, OUT-4102-65 (November 1996), hep-th/9612012.
- [14] D. Bar-Natan, Topology 34,2 (1995) 423.
- [15] D.J. Broadhurst, D. Kreimer, *Feynman Diagrams as a Weight System: Four-Loop Test of a Four-Term Relation*, OUT-4102-66, MZ-TH/96-37, hep-th/9612011.
- [16] P. D. Jarvis, A. Kalloniatis, G. Thompson, I. Tsohantjis, Mod. Phys. Lett.**A11** (1996) 1095.
- [17] D. Kreimer, *Knots and Feynman Diagrams* (Cambridge University Press, in preparation).
- [18] D. Zagier, in Proc. First European Congress Math. (Birkhäuser, Boston, 1994) Vol II, pp 497-512; *Multiple Zeta Values*, in preparation.